J Mater Sci (2008) 43:5131–5138
DOI 10.1007/s10853-008-2737-4

Thermal properties of multicomponent tellurite glass

R. El-Mallawany · I. Abbas Ahmed

Received: 23 February 2008 / Accepted: 16 May 2008 / Published online: 7 June 2008

Abstract Quaternary tellurite glass systems of the form $80TeO_2$–$5TiO_2$–$(15 - x)WO_3 - xA_nO_m$ where A_nO_m is Nb_2O_5, Nd_2O_3, and Er_2O_3, $x = 0.01$, 1, 3, and 5 mol% for Nb_2O_5 and $x = 0.01$, 0.1, 1, 3, 5, and 7 mol% for Nd_2O_3 and Er_2O_3, have been prepared by the melt quenching. Density and molar volumes have been measured and calculated for every glass system. The thermal behavior of the glass series was studied by using the differential thermal analysis DSC. Glass transition temperature T_g, crystallization temperature T_c, and the onset of crystallization temperature T_x were determined. The glass stability against crystallization S ($\approx$100 °C) and glass-forming tendency K_g ($\approx$0.3) have been calculated. Specific heat capacity C_p ($\geq$1.4 J/g °C) was measured from room temperature and above the T_g for every composition in each glass series. Quantitative analysis of the above thermal properties of these new tellurite glass with the structure parameters like average cross-link density $\bar{n}_c$ ($\geq$2.4), number of bonds per unit volume n_b ($\geq 8 \times 10^{28}$ cm^{-3}), and the average stretching force constant (F) have been studied for every glass composition.

Introduction

Tellurite glasses are of scientific and technological interest because of their high refractive indices, low melting temperatures, high dielectric constants as well as their good UV and IR transmissions. Recently, they have been considered as promising materials for non-linear optical devices [1]. Educationally, an introduction to "Tellurite Glasses" lecture has been provided as resource for the entire international glass community available in video streaming format on the IMI website [2]. Some tellurite glasses are also reported to be suitable for setting up optical fiber amplifiers [3], they also are of usual electronic behavior-notable semiconductivity and electronic switching effects [4]. Tellurite glasses have attracted a great deal of attention both in fundamental research and also in optical devices fabrication over the past several years. It is mainly because the optical glasses based on tellurite are showing good transparency in the visible–infrared, relatively low phonon energy compared with other oxide glasses such as silicate and phosphate glasses, large resistance against corrosion, and the possibility to incorporate a large amount of rare earth. In addition, tellurite glasses could be used in production of fiber, planer broadband amplifiers, and lasers [5]. These special optical properties encourage identifying them as important materials for potential applications in high performance optics, laser technology, and optical communication networks. Tungsten–tellurite glass is proposed as a host for broadband erbium-doped fiber amplifiers (EDFA) [6]. Near-infrared emissions with widely different widths in two kinds of Er^{3+}-doped oxide glasses (alkali–barium–bismuth–tellurite) with high refractive indices and low phonon energies have been achieved [7]. Very recently [8], the refractive index and UV spectra of the quaternary tellurite glass system of the form $80TeO_2$–$5TiO_2$–$(15 - x)WO_3 - xA_nO_m$ where A_nO_m is Nb_2O_5, Nd_2O_3, and Er_2O_3, $x = 0.01$, 1, 3, and 5 mol% for Nb_2O_5 and $x = 0.01, 0.1, 1, 3, 5$, and 7 mol% for Nd_2O_3 and Er_2O_3. The refractive index has been measured at room

R. El-Mallawany (✉)
Physics Department, Faculty of Science, Menofia University, Menofia, Egypt
e-mail: relmallawany@hotmail.com

I. A. Ahmed
Supreme Education Council, Doha, Qatar

temperature and at wavelengths 486.13, 587.56, 589, and 656.27 nm. The average dispersion ($n_F - n_C$), and Abbe number of this glass were estimated. The UV spectra of the glasses have been measured in the wavelength range of 200–1000 nm at room temperature. The relation between the refractive index and optical energy gap is examined. The purpose of the present paper is to complete the previous study [8] by examining and analyzing the thermal behavior of the same glass samples to get a complete view about the optical and thermal properties of tellurite glass.

Experimental procedure

Quaternary tellurite glass systems of the forms $80TeO_2$–$5TiO_2$–$(15 - x)$ $WO_3 - xA_nO_m$ where A_nO_m is Nb_2O_5, Nd_2O_3, and Er_2O_3, $x = 0.01$, 1, 3, and 5 mol% for Nb_2O_5 and $x = 0.01$, 0.1, 1, 3, 5, and 7 mol% for Nd_2O_3 and Er_2O_3, were prepared by the melt quenching method. The batches of high purity constituents were thoroughly mixed and grounded in agate mortar. The powdered mixture was then put in an alumina crucible and heated in an electric furnace in air atmosphere. In order to reduce any tendency of volatilization the mixture was kept at 300 °C for 15 min. Depending upon the batch material the temperature was set in the range of 750–850 °C, the melt was left in this range for 30 min to assure complete melt of the constituents and it was stirred a few times to improve the homogeneity. The melt which had a high viscosity, was then cast at room temperature in a stainless steel mold of dimension $1 \times 1 \times 1$ cm^3. Subsequently, the sample was transferred to an annealing furnace and kept for 1 h at 300 °C. Then the furnace was switched off and the glass sample was allowed to cool inside for 24 h. The prepared cubic samples were polished by a lapping machine with 600 grade and soft fine AlO_3 powder. Opposite faces were finished optically flat and parallel with a high mirror-like surface.

The density of the prepared glass samples were determined at 20 °C temperature by a simple Archimedes's method using distilled water as an immersing liquid of density ($\rho = 0.998207$ g/cm^3) and a digital balance of sensitivity 10^{-4} g. Glass transition temperature T_g, crystallization temperature T_c, and the onset of crystallization temperature T_x were determined by using the recorded thermograms of the differential scanning calorimetry (DSC) Perkin–Elmer 7 at 10 °C/min heating rate. Specific heat capacity C_p is measured with (DSC-7 Perkin Elmer) equipped with a computerized data acquisition and system analysis. Samples for heat capacity were typically 30–50 mg in mass enclosed in crimped Al DSC pans. The C_p was measured from room temperature and above the T_g.

Results and discussion

Glass series, densities, and molar volume

The prepared quaternary tellurium glass has different colors ranging from yellowish to reddish brown depending on the ions modifier percentage. They are all transparent and homogenous. The prepared samples were carefully checked for any air pockets/bubbles and only those which were free from these defects, were chosen for further investigation. The results of the glass densities measurements are presented in Fig. 1 for the three prepared quaternary glass series:

$$80TeO_2–5TiO_2–(15 - x)WO_3 - xNb_2O_5, \quad (a)$$

$$80TeO_2–5TiO_2–(15 - x)WO_3 - xNd_2O_3, \quad (b)$$

$$80TeO_2–5TiO_2–(15 - x)WO_3 - xEr_2O_3, \quad (c)$$

where $x = 0.01$, 0.1, 1, 3, 5, and 7 mol%.

Measurements have been made for the variation of the densities of the three quaternary systems with mol% increase of the modifiers Nb_2O_5, Nd_2O_3, Er_2O_3 at the expense of WO_3 mol%. Their densities were found to vary in the range (5.178–5.989 g/cm^3). These values are less than the tellurite-based quaternary system reported by [9], but higher than the ternary tellurite-based series prepared by [10] and much higher than the density of SiO_2 glass reported by [11]. Comparison with the pure TeO_2 glass of density (5.11 g/cm^3) [12] has been made and it was found to be higher but close to the value of binary tellurite-based glass [13]. A systematic variation of the densities with the modifiers content reflects the good mix and thermal treatment of corresponding melts and samples. Referring to the (a) series Fig. 1 shows an increase of the glass density from

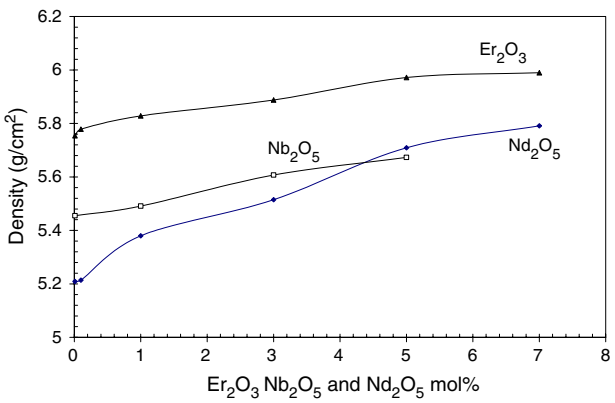

Fig. 1 Variation of the density of the quaternary tellurite glass system doped with Nb_2O_5 Nd_2O_3, and Er_2O_3 mol%

(5.455 g/cm^3 to 5.673 g/cm^3) with increasing mol% of the modifier (Nb_2O_5) from (0.01 to 5 mol%). The (b) series densities were found to range from (5.178 g/cm^3 to 5.791 g/cm^3) with the mol% increase of the modifier (Nd_2O_3) from (0.01 to 7 mol%) as shown in Fig. 1. For the (c) series the densities were found to increase from (5.775 g/cm^3 to 5.989 g/cm^3) with the percentage increase of the modifier (Er_2O_3) from (0.01to 7 mol%) as shown in Fig. 1. The observed systematic increase of the density values with contents of ions modifiers in the three series are attributed to the substitution of WO_3 of molecular weight 231.84 g/mol with higher molecular weight modifiers (Nb_2O_5) of molecular weight 265.81 g/mol, rare earth metal (Nd_2O_3) of molecular weight 336.48 g/mol, and (Er_2O_3) of molecular weight 382.518 g/mol in the glass network. One of the clear factors in controlling the density of the three glass series, is the direct substitution of WO_3 with higher molecular mass modifiers Nb_2O_5, Nd_2O_3, and Er_2O_3, resulting in high glass density, and consequently partially controlling the bulk properties of the glass such as in the linear refractive index [8].

The molar volume for the three series was calculated using the equation:

$$V = \frac{M_G}{\rho_G} \quad (1)$$

where V is the molar volume, M_G is the glass formula weight, and ρ_G is the glass density. The molar volumes for the three glass series were found in the range (28.82–32.19 cm^3). For the (a) series the molar volume was found to be decreased from (30.51 to 29.63 cm^3) as the result of the increase of the modifier (Nb_2O_5) from (0.01to 5 mol%) as shown in Fig. 2 and for the (b) series it was found to be decreased from (32.19 to 29.99 cm^3) as a result of the increase of the modifier (Nd_2O_3) from (0.01 to 7 mol%) as shown in Fig. 2. On the other hand, in contrast to series (a) and (b) a direct proportional relation between the molar volume and the mol% increase of the modifier (Er_2O_3) was found to exist in series (c). The molar volume was found to be increased from (28.82 to 32.19 cm^3) as the content of modifier (Er_2O_3) increased from (0.01 to 7 mol%) as shown in Fig. 2.

By looking at the relative mol% increase of the formula weights for the (a) and (b) series shown in Table 1 resulting from an increase of the modifiers (Nb_2O_5, Nd_2O_3) mol%, are less compared with the relative percentage increase of the corresponding glass densities. So, the observed decrease of the molar volume with the increase of the glass density is attributed to the role and participation of Nb_2O_5 and Nd_2O_3 in the network structure, contribute toward creating more compact glass network. This leads to the observed inverse relation between the molar volume and the glass density. In contrast to the roles of Nb_2O_5 and Nd_2O_3 as network modifier, Er_2O_3 tends to create more open glass network structure, and correspondingly the molar volume increases with increasing Er_2O_3 mol%. Common glass-forming oxides have less density but more free volume than the corresponding crystalline forms, because glass has a more open network structure. So, it is more informative to compare the ratio of densities of pure TeO_2 glass (5.105 g/cm^3) and that of the corresponding crystalline forms (5.99 g/cm^3) [14]. The ratio equal to 1.17 and the free volume is 4.66 cm^3, i.e., the change is only (17.5%) from crystalline solid to be non-crystalline solid. Hence, the fact that the molar volume of the glass is greater than that of the crystal which correlates extremely well with longer number of TeO_2 units that can be accommodated in the more open structure of the vitreous state.

Thermal properties of tellurite glass

Glass transition temperature (T_g)

For the (a) series the glass transition temperature (T_g) increases from 396 to 405 °C as shown in Fig. 3 as a result

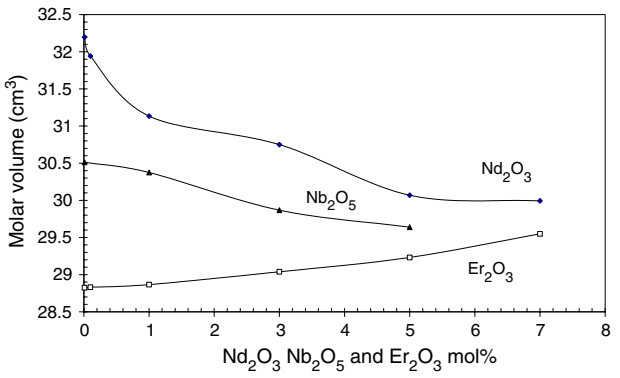

Fig. 2 Variation of the Molar volumes of the quaternary tellurite glass system doped with Nb_2O_5 Nd_2O_3, and Er_2O_3 mol%

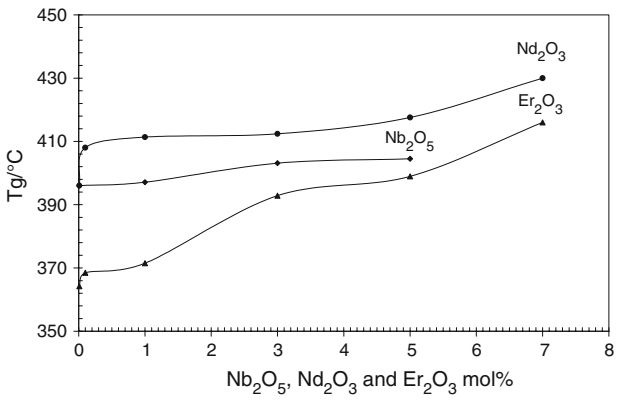

Fig. 3 Variation of T_g for the quaternary tellurite doped with Nd_2O_3, Nb_2O_5, and Er_2O_3 mol%

of increasing of Nb_2O_5 content from (0.01 to 5 mol%). These values of (T_g) are close to the ternary tellurite-based glasses [15]. The observed increase of (T_g) with the content of the Nb^{+5} ions is due to the ability of these ions to strongly combine the structural units by exerting strong columbic interaction with the surrounding oxygen of the network [16]. For the (b) and (c) series, the (T_g) increases from (396 to 430 °C) and from (364 to 416 °C) as the contents of Nd_2O_3 and Er_2O_3 increases from (0.01 to 7 mol%), respectively, Fig. 3. To explain the noticeable increase of (T_g) with Nd_2O_3 and Er_2O_3 contents are due to the partial substitution of WO_3 by these oxides of greater number of cations per mol and average cross-link density. This consequently, leads to an increase of the number of bonds per unit volume, which has a direct proportional relation with (T_g).

The glass transition temperature for pure tellurium dioxide (TeO_2) was measured by [12] and found to be 325 °C. The low (T_g) value for pure tellurite glass compared with (T_g) for the three prepared glass series which indicates that the glass networks formed by these systems are stronger than the pure substance, this will confirm the role of transition metal (T.M.O) oxides TiO_2 and WO_3 in forming the glass series as conditional glass network former as well as the role of the modifiers in forming a stable glass network with TeO_2 as host material.

The glass transition temperature (T_g) depends on a number of parameters. It increases with the increasing of the average cross-linking of the network and the strength of the bonds of which it is composed, i.e., $T_g = f(\bar{n}_c, f)$[10, 11, 12, 17]. It is more informative for analyzing the glass network to correlate data between thermal and structural properties, e.g., between (T_g) and average cross-link density ($\bar{n}_c$), number of bonds per unit volume (n_b), and the average stretching force constant (F).

To do further quantitative analysis relating the structure parameters on (T_g) the average cross-link density was calculated using the relation:

$$\bar{n}_c = \frac{\sum_i x_i (n_c)_i (N_c)_i}{\sum_i x_i (N_c)_i} \tag{2}$$

where x is the mol fraction of component oxide, n_c is the cross-link density per cation, N_c is the number of cations per glass formula unit, and i denote the component oxide. The increase of Nb_2O_5, Nd_2O_3, and Er_2O_3 concentration on the expense of WO_3 from (0.01 to 7 mol%) leads to an increase in the average cross-link density from (2.40 to 2.50) as shown in Table 1 for the three series is consistent with the (T_g) increases shown in Fig. 3.

The number of bonds per unit volume (n_b) of the glass for the three series was calculated using the relation:

Table 1 Glass composition, formula weight, and average cross-link density ($\bar{n}_c$)

Glass composition	Formula weight (g/mol)	Average crosslink density ($\bar{n}_c$)
TeO_2–TiO_2–WO_3– Nb_2O_5		
80–5–14.99–0.01	166.452	2.40
80–5–14–1	166.788	2.42
80–5–12–3	167.467	2.45
80–5–10–5	168.147	2.48
TeO_2–TiO_2–WO_3–Nd_2O_3		
80–5–14.99–0.01	166.459	2.40
80–5–14.90–0.1	166.553	2.40
80–5–14–1	167.495	2.42
80–5–12–3	169.587	2.45
80–5–10–5	171.681	2.48
80–5–8–7	173.773	2.50
TeO_2–TiO_2–WO_3–Er_2O_3		
80–5–14.99–0.01	166.461	2.40
80–5–14.90–0.1	166.596	2.40
80–5–14–1	167.952	2.42
80–5–12–3	170.966	2.45
80–5–10–5	173.979	2.48
80–5–8–7	176.993	2.50

$$n_b = \frac{N_A}{V_m} \sum_i (n_f x)_i \tag{3}$$

where x is the mol fraction of component oxide, N_A Avogadro's number, V_m is the molar volume of the glass, n_f is the coordination number of the cations, and i denotes the component oxide.

The number of bonds per unit volume was found to increase with increasing mol% of the modifier in the (a), (b), and (c) series from (8.68×10^{28} to 9.55×10^{28} m^{-3}), from (8.24×10^{28} to 9.67×10^{28} m^{-3}), and from (9.19×10^{28} to 9.82×10^{28} m^{-3}), respectively, as shown in Fig. 4. Comparing these values with the number of bonds per unit volume of pure TeO_2 glass of value (7.74×10^{28} m^{-3}) obtained by [12] will reflect the more bonded quaternary glass network.

The average stretching force constants (F) of the glass for the three series were calculated using the relation 4 and 5 given by [10–12, 18]:

$$f = \frac{17}{r^3} \tag{4}$$

$$F = \frac{\sum (x n_f f)_i}{\sum (x n_f) i} \tag{5}$$

where x is the mol fraction of component oxide, n_f is the coordination number of cation, (f) is the stretching force

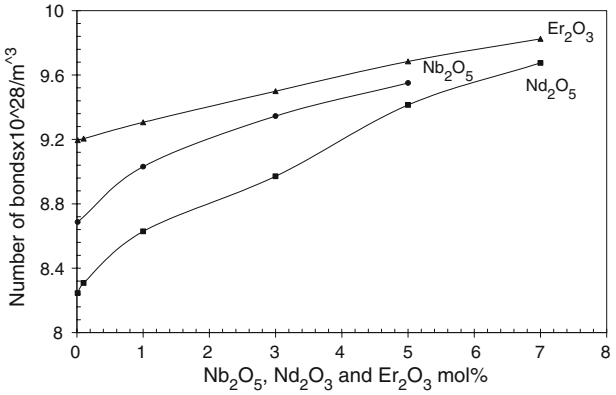

Fig. 4 Variation of the number of bonds per unit volume for the quaternary tellurite doped with Nd_2O_3, Nb_2O_5, and Er_2O_3 mol%

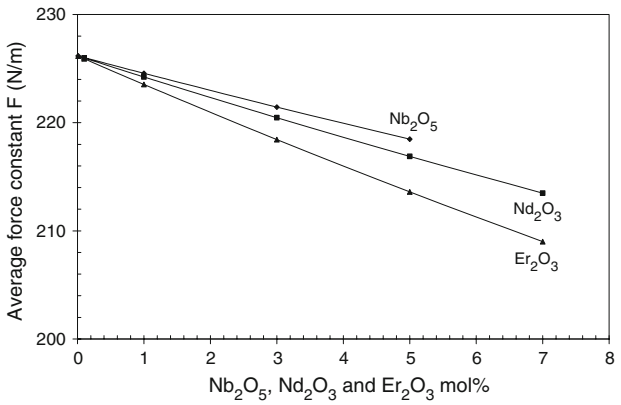

Fig. 5 Variation of the average force constant for the quaternary tellurite doped with Nd_2O_3, Nb_2O_5, and Er_2O_3 mol%

constant of oxide and *i* denotes the component oxide, and (*r*) is the cation radius in Angstrom.

By using the bond length of each cation–anion bond (*r*) in every oxide used in the present multicomponent tellurite glass from reference [19], the average stretching force constant (*F*) was found to increase with the increasing mol% of the modifier in the (a), (b), and (c) series from (218.47 to 226.16 N/m), from (213.48 to 226.23 N/m), and from (209 to 226.15 N/m), respectively, shown in Fig. 5. While the value of (*F*) for pure TeO_2 is 216 N/m [12]. From the previous analysis, we deduce that the average stretching force constant in the three glass series is acting toward decreasing the (T_g) with increasing mol% modifier, but in contrast, the average cross-link density and number of bonds per unit volume are acting in the opposite direction, i.e., toward increasing the (T_g) with increasing mol% modifier. By looking to the experimental results of the (T_g) Fig. 3 it is obvious that the combined effect of both the cross-link density and number of bonds per unit volume as an increasing parameters on (T_g) overwhelms the decreasing effect of the average stretching force constant. Finally, we conclude that these new glass systems are more linked than the pure TeO_2 glass and consequently lead to the observed increase of (T_g) with the mol% of the modifiers in the three series.

Specific heat capacity

Measurements of the temperature variation of the specific heat capacity have been a rich source of information on electronic, atomic, and molecular dynamics of solids. The DSC (Differential Scanning Calorimetry) was used to obtain thermal scanning curves for measuring the specific heat capacity of the three glass series, in the range between 100 °C and 550 °C, allowing the glass transition temperature (T_g) to be measured. All samples from the three series show clear glass transition as in Fig. 6a, b, and c.

In most samples the crystallization temperature (T_c) does not appear in DSC traces, as it is higher than 550 °C, but it shows up in one sample 7 mol% Er_2O_3 with clear exothermic peak at (T_c = 490 °C). An approximate relation for evaluation of the melting point (T_m) may be found by applying the classical two-third rule expressed as (T_g/T_m) = 2/3 as in reference [20].

The thermal stability range (S) for the glass can be estimated using the relation:

$$S = (T_c - T_g) \tag{6}$$

This provides a good estimate of the tendency of the glass to crystallize. It should usually be larger than 100 °C to obtain thick glass samples. The stability of most prepared samples were found using relation 6 and they were greater than 100 °C except one sample (7 mol% Er_2O_3) in Fig. 7 and its stability range was found to be equal to 74 °C. The observed low stability in this sample indicates that this glass network is close to the boundaries of the formation range. To perform further thermal stability criterion on this particular sample the glass-forming tendency (K_g), which is a useful devitrification tendency measure for the glass, is given by:

$$K_g = \frac{T_c - T_g}{T_m - T_c} \tag{7}$$

The larger (K_g), the stronger is the inhibition to nucleation and crystallization processes, and consequently, the larger the thermal stability of the glass. Low value of K_g indicates high tendency to devitrify. Understanding the thermal stability makes possible the development and use of TeO_2-based glasses as non-linear optical martial or matrix glass for rare earth elements [21]. The value of (K_g) for the 7 mol% Er_2O_3 was found to be 0.3 compared to 0.41 for pure TeO_2 [16]. It is higher than the binary TeO_2–La_2O_3 of range value (0.21–0.25) [22] but close to the binary system 92 TeO_2–8Co_2O_4 of value (0.31), and lower than the binary system 80 TeO_2-20 MoO_3 [17].

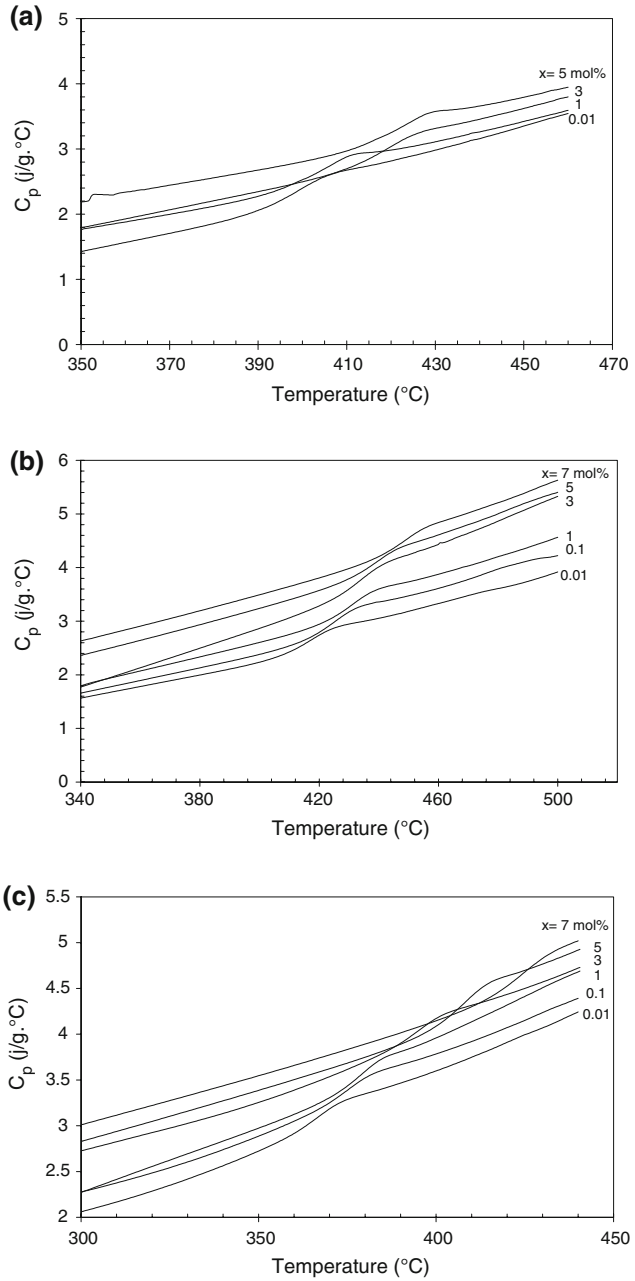

Fig. 6 (**a**) Variation of the specific heat capacity C_p for the quaternary tellurite doped $x = 0.01$, 1, 3, and 5 mol% of Nb_2O_5 in the temperature range 350–470 °C. (**b**) Variation of the specific heat capacity C_p for the quaternary tellurite doped with $x = 0.01$, 0.1, 1, 3, 5, and 7 mol% of Nd_2O_3 in the temperature range 340–500 °C. (**c**) Variation of the specific heat capacity C_p for the quaternary tellurite doped with $x = 0.01$, 0.1, 1, 3, 5,7 Er_2O_3 mol% in the temperature range 300–450 °C

The specific heat capacities (C_p) for all prepared samples were found to increase with temperature. For the (a) series the specific heat capacity of the glass state (C_{pg} at 380 °C) increases from (1.86 to 2.56 J/g °C) and at the super-cooled liquid state (C_{pl} at 460 °C) increases from (3.54 to 3.94 J/g °C) with increasing of the modifier

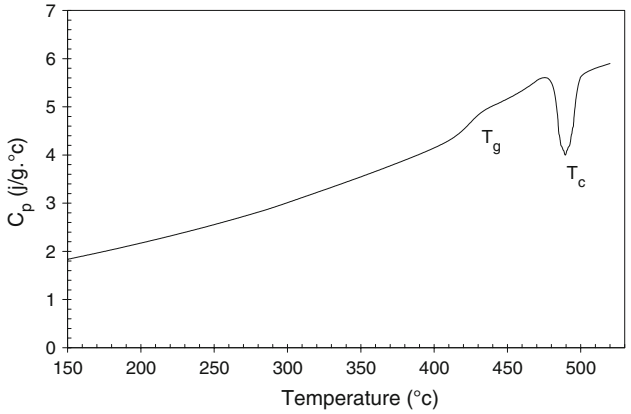

Fig. 7 Variation of the specific heat capacity C_p for the quaternary tellurite doped with 7 mol% Er_2O_3 in the temperature range 150–500 °C

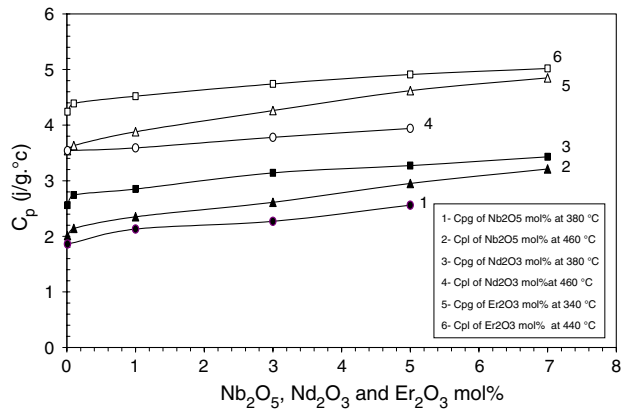

Fig. 8 Variation of specific heat capacity at glassy state (C_{pg}) and super-cooled liquid (C_{pl}) for the quaternary tellurite doped with Nb_2O_5, Nd_2O_3, and Er_2O_3 mol%

(Nb_2O_5) from (0.01 to 5 mol%) Fig. 8. For the (b) series (C_{pg} at 380 °C) increases from (2.01 to 3.21 J/g °C) and (C_{pl} at 460 °C) increases from (3.54 to 4.85 J/g °C) with the increasing of the modifier (Nd_2O_3) content from (0.01 to 7 mol%) Fig. 8. For the (c) series the (C_{pg} at 340 °C) increases from (2.56 to 3.43 J/g °C) and (C_{pl} at 440 °C) increases from (4.24 to 5.02 J/g °C) with the increasing of the modifier (Er_2O_3) content from (0.01 to 7 mol%) Fig. 8.

These results (C_p) were higher than the reported values of the (C_p) of ternary-based tellurite glass [23], and of the binary vanadium tellurite glass of the form $(100-x)$ mol% TeO_2-x mol% V_2O_5. The values of C_{pg}, are in the range (0.76–1.45 J/g K^{-1}), and the values of C_{pl}, are in the range (1.0–2.12 J/g °C) [24]. To explain the noticeable increase of the (C_p) values for the three series with modifier content at the expense of WO_3, is attributed to the increasing number of oscillators as the result of substitution of Nb_2O_5 (seven particles), Nd_2O_3 (five particles), and Er_2O_3 (five particles) for WO_3 (particles four).

To shed more light on the structure of tellurite glass, further analysis of the behavior of the (C_p) in the transition range between the super-cooled liquid and glassy state, i.e., (C_{pl}/C_{pg}) have been found as well as (ΔC_p), (i.e., C_{pl}-C_{pg}) for all samples. In general, the so called strong liquids have a tendency toward small changes in (C_p) values at (T_g), i.e., $C_{pl}/C_{pg} \approx 1.1$, compared with fragile liquids which are easily devitrified with $C_{pl}/C_{pg} > 1.1$. The viscous-flow behavior at elevated temperature of the TeO_2 can be explained by change to the basic crystal structure comprising of trigonal bipyramid units, that are present in the glass at room temperature, to TeO_3 trigonal pyramid units with non-bridge oxygen (NBO) atoms as the temperature increased above (T_m) [25, 26]. Such structural change above the glass transition causes a large change in viscous-flow behavior.

Liquid with low (ΔC_p) values, such as SiO_2, have generally tetrahedral coordinated network structures that are expected to experience relatively little disruption during heating. In contrast, liquids with large (ΔC_p) values have intermediate–range structures that are expected to change substantially as the temperature increases. For the (a) series the ratio of (C_{pl}/C_{pg}) and (ΔC_p) Figs. 9 and 10 were found to decrease from (1.9 to 1.54) and from (0.387 to 0.287), respectively, with increasing of the (Nb_2O_5) content from (0.01 to 5 mol%). For the (b) series the ratio of (C_{pl}/C_{pg}) decreases from (1.76 to 1.51 J/g °C) and (ΔC_p) from (0.472 to 0.3) as the content of Nd_2O_3 increases from (0.01 to7 mol%) as shown in Figs. 9 and 10. The behavior of both series (a) and (b) indicates that increasing the modifier content forms less fragile liquids.

This is because the (C_{pl}/C_{pg}) and (ΔC_p) are decreasing functions of the modifier content.

The reported value of the (C_{pl}/C_{pg}) of the glass system (20−x) mol% Li_2O − x mol% Na_2O-80 mol% TeO_2 was included in the category of fragile liquids as mentioned by [27]. Also, Zahra and Zahra [28] reported that TeO_2-based

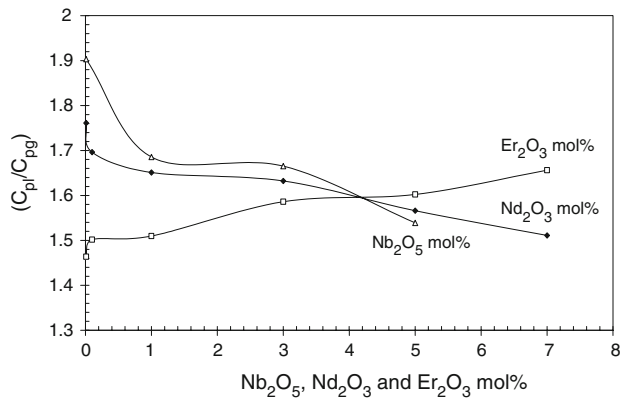

Fig. 9 Variation of the ratio (C_{pl}/C_{pg}) for the quaternary tellurite doped with Nb_2O_5, Nd_2O_3, and Er_2O_3 mol%

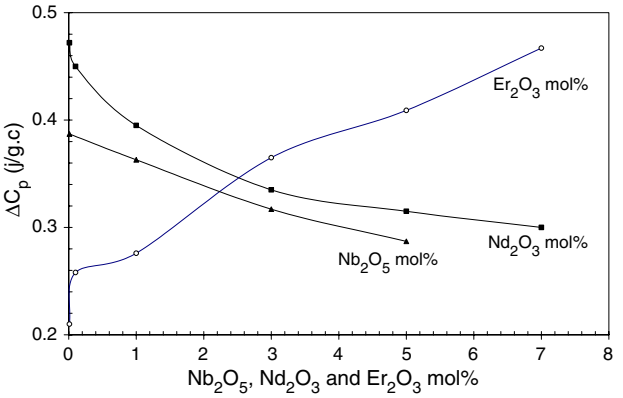

Fig. 10 Variation of ΔC_p for the quaternary tellurite doped with Nb_2O_5, Nd_2O_3, and Er_2O_3 mol%

samples containing TlO0.5, AgO0.5, or AgI have large values of (C_{pl}/C_{pg}) (1.43–1.66). For the (c) series the ratio of (C_{pl}/C_{pg}) was found to be increased from (1.46 to 1.65) whereas delta C_p increased from (0.21 to 0.46 J/g °C) as the modifier (Er_2O_3) content increased from (0.01% to 7 mol%) as shown in Figs. 9 and 10. This suggests that this series belongs to the category of fragile liquids and therefore, by increasing the modifier contents it will results in pushing toward more fragility.

Conclusions

Quaternary tellurite glass were prepared and investigated for the thermal properties. The thermal properties: glass transition temperature T_g, crystallization temperature T_c, the onset of crystallization temperature T_x, glass stability against crystallization S and glass-forming tendency K_g, specific heat capacity C_p were measured and quantitatively analyzed.

- The decrease in molar volumes indicates that Nb_2O_5 and Nd_2O_3 modifiers have been accommodated in the glass structure, and have created a more compact glass network. In contrast, the molar volume increases as the content of the modifier Er_2O_3 increases. Although Er_2O_3 has the highest density glass among the studied modifiers, it is accommodated in the more open structure of the glassy state.
- These glass samples possess high thermal stability greater than the 100 °C required by the thermal stability criteria. Hence, all the studied samples are promising candidates for rare-earth-doped optical fiber, with one glass sample exception (7 mol% Er_2O_3) due to its low thermal stability 74 °C and Hurby's criterion of value 0.3.
- The recorded increase of the glass transition temperature with the content of the modifier is attributed to the increase in the cross-link density and the number of

bonds per unit volume in the glass. Glass networks formed in the prepared samples are stronger than that of the pure host material TeO_2 alone. This is inferred directly from the increasing values of (T_g) with modifier percentages and it finds direct support through the quantitative calculations of the number of bonds per unit volume, the cross-linked density and the average stretching force constant.

- Theoretical calculations of the number of bonds per unit volume revealed the following: increases of the Nb_2O_5 concentration leads to an increase in number of bonds per unit volume. The average stretching force constant was found to increase with the increasing mol% of the modifiers which explain quantitatively the decrease of the glass transition temperature of the present tellurite glasses.
- Large values of specific heat capacity C_p have been observed compared to silicate glasses. Calculations of the ratios of the specific heat capacities of the super-cooled liquid to that at the glassy state revealed that these glass samples belong to the category of fragile liquids.

References

1. El-Mallawany R (2002) Tellurite Glasses, Physical Properties & Data, CRC Press
2. International Materials Institute for New Functionality in Glass (IMI-NFG) (2005) Lehigh University, USA. http://www.lehigh.edu/imi/resources.htm
3. Wang J, Vogel E, Snitzer E (1994) Opt Mater 3:187
4. Hirashima H, Youshida M (1986) J.Non-Cryst Solids 86:327
5. Chen D, Liu Y, Zhang Q, Deng Z, Jiang Z (2005) Mater Chem Phys 90:78
6. Shen S, Naftaly M, Jha A (2002) Opt Commun 205(1–3):101
7. Lin H, Tanabe S, Lin L, Hou YY, Liu K, Yang DL, Ma TC, Yu JY, Pun EYB (2007) J Lumin 124:167
8. El-Mallawany R, Dirar Abdalla M, Abbas Ahmed I (2008) J Mater Chem Phys 109:291–296
9. El-Mallawany R, Saunders G (1988) J Mater Sci Lett 6:443
10. Bridge B (1987) Phys Chem Glasses 28:70
11. Bridge B, Patel N, Waters D (1983) Physica Status Solidi A 77:655
12. Lambson E, Saunders G, Bridge B, El-Mallawany R (1984) J Non-Cryst Solids 69:117
13. AL-Ani S, Hogarth C (1987) J Mater Sci Lett 6:519
14. Havinga E (1961) J Phys Chem Solids 18:253
15. Stanworth J (1952) J Soc Glass Technol 36:217
16. Komatsu T, Tawarayama H, Mohri H, Matusita K (1991) J Non-Cryts Solids 135:105
17. El-Mallawany R (1995) J Mat Sci Mater Electron 6:1
18. Bridge B, Higazy A (1986) Phys Chem Glasses 27:1
19. Walls AF (1975) Structure of inorganic compounds, 4th edn. Clarendon Press, London, pp 452, 455, 582
20. Klouche Bouchaour ZC, Poulain M, Belhadji M, Hager I, El Mallawany R (2005) J Non-Cryst Solids 351:818–825
21. Zhang J, Qiu J, Kawamoto Y (2002) Mater Lett 55:77–82
22. EL-Koshkhany N (2002) Ph.D. Thesis, Faculty of Science, Menofia University, Menofia, Egypt
23. Kosuge T, Benino Y, Dimitrov V, Sato R, Komatsu T (1998) J Non-Cryst Solids 242:154–164
24. El -Mallawany R (2000) Physica Status Solidi 177:439–443
25. Kowada Y, Habu K, Adachi H, Tatsumisago M, Minami T (1992) Chem Express 17:965
26. Tatsumisago M, Lee S, Minami T, Kowada Y (1994) J Non-Cryst Solids 177:154–163
27. Komatsu T, Noguchi T (1997) J Am Ceram Soc 80:1327–1332
28. Zahra C, Zahra A (1995) J Non-Cryst Solids 190:251–257